Author/s:
Louis, C;Ngo, D;D'Silva, DB;Hansen, J;Phillipson, L;Jousset, H;Novello, P;Segal, D;Lawlor, KE;Burns, CJ;Wicks, IP

Title:
Therapeutic Effects of a TANK-Binding Kinase 1 Inhibitor in Germinal Center–Driven Collagen-Induced Arthritis

Date:
2019-01-01

Citation:
Louis, C., Ngo, D., D'Silva, D. B., Hansen, J., Phillipson, L., Jousset, H., Novello, P., Segal, D., Lawlor, K. E., Burns, C. J. & Wicks, I. P. (2019). Therapeutic Effects of a TANK-Binding Kinase 1 Inhibitor in Germinal Center–Driven Collagen-Induced Arthritis. Arthritis and Rheumatology, 71 (1), pp.50-62. https://doi.org/10.1002/art.40670.

Article type : Full Length

Article type: Full-length

Therapeutic effects of a TBK1 kinase inhibitor in germinal center-driven, autoantibody-mediated inflammatory arthritis

Cynthia Louis PhD[1,5], Devi Ngo PhD[1,5], Damian B D'Silva[1,5], Jacinta Hansen[1,5], Louisa Phillipson PhD[2,5], Helene Jousset PhD[3,5], Patrizia Novello[3,5], David Segal PhD[4,5], Kate E Lawlor PhD[1,5], Christopher J Burns PhD[2,5,6], Ian P Wicks PhD[1,5,7]

[1]Inflammation Division, [2]Chemical Biology Division, [3]Systems Biology and Personalised Medicine Division, and [4] Cancer and Haematology Division, The Walter and Eliza Hall Institute of Medical Research, Parkville, VIC, 3052, Australia;
[5] Department of Medical Biology, The University of Melbourne, Parkville, VIC, 3010, Australia
[6] School of Chemistry, The Bio21 Institute, The University of Melbourne, VIC 3010, Australia.
[7] Rheumatology Unit, Royal Melbourne Hospital, Parkville, VIC, 3050, Australia

Running title: Targeting GC using TBK1 inhibitor in CIA

To whom correspondence should be addressed:
Prof. Ian Wicks
The Walter and Eliza Hall Institute of Medical Research
Inflammation Division
1G Royal Parade, Parkville, VICTORIA 3052, Australia
wicks@wehi.edu.au

ABSTRACT

Objective

The production of class-switched high-affinity autoantibodies derived from organised germinal centers (GC) is a hallmark of many autoimmune inflammatory diseases, including rheumatoid arthritis (RA). TANK-binding kinase 1 (TBK1) is a serine-threonine kinase involved in the maturation of GC T follicular B helper cells (T_{FH}) downstream of inducible T cell costimulator (ICOS) signalling. We therefore assessed the therapeutic potential of TBK1 inhibition using a small molecule inhibitor – known as WEHI-112 – in antibody dependent models of inflammatory arthritis.

Methods and Results

WEHI-112 - a tool compound, which is semi-selective for TBK1, but also has activity against IKKε and JAK2 - abolished TBK1-dependent IRF3 activation and inhibited type I IFN responses *in vitro*. *In vivo*, treatment with WEHI-112 selectively abrogated clinical and histological features of established, antibody-dependent collagen-induced arthritis (CIA), but had minimal effects on an antibody-independent model of antigen-induced arthritis (AIA) or on K/BxN serum transfer-induced arthritis (STIA). In keeping with these findings, WEHI-112 reduced arthritogenic collagen type II (CII)-specific IgG1 and IgG2b antibody production. Furthermore, WEHI-112 altered the GC T_{FH} phenotype and GC B cell function in CIA.

Conclusion

In summary, we report that TBK1 inhibition using WEHI-112, albeit semi-selective for TBK1, abrogated antibody-dependent CIA, most likely explained by targeting TBK1-mediated mechanisms in the GC reaction as its major effect. This approach may have therapeutic potential in RA and in other GC-associated autoantibody-driven inflammatory diseases.

INTRODUCTION

The presence of high-affinity autoantibodies, such as anti-citrullinated peptide autoantibodies (ACPAs) in rheumatoid arthritis (RA) [1] and anti-nuclear autoantibodies (ANAs) in systemic lupus erythematosus (SLE) [2] is a common feature of humorally mediated autoimmune diseases and has been linked to the induction of autoimmune inflammation [3, 4]. The pathogenicity of high-affinity autoantibodies is exemplified in the K/BxN serum transfer-induced arthritis model of RA [5]. Transfer of serum or purified autoantibodies generated from autoimmune K/BxN transgenic arthritic mice alone is sufficient to induce arthritis in naive recipients [5]. Key cytokines, such as TNF-α and IL-1β, are downstream amplifiers of joint inflammation in this model [6].

Germinal center (GC) formation in secondary lymphoid tissues plays a major role in humoral autoimmunity [7]. In the inductive phase of an antibody response, GC T follicular B helper cells (T_{FH}) cells and GC B cells cooperate to mediate immunoglobulin class-switching, affinity selection and the generation of GC-derived memory B cells and antibody-

secreting plasma cells. GC reactions, including cytokines produced by Th17 cells within the GCs, also induce post-translational modification of antibodies produced by recently generated, GC-derived plasma cells and thereby influence the pathogenicity of arthritogenic autoantibodies in the autoimmune collagen-induced arthritis (CIA) model [8].

Biological therapies to deplete B cells and antagonize key inflammatory cytokines such as TNF, have been employed clinically with success in treating RA. Small molecule kinase inhibitors targeting Janus kinases (JAK inhibitors/Jakinibs) have also been approved for RA [9]. Nevertheless, important challenges remain in the treatment of RA. Responsiveness to these therapies varies in different patients, reflecting the heterogeneity of underlying pathogenic mechanisms and stage of disease. Additionally, TNF antagonism and Jakinibs exert effects on the immune response that increase the risk of infection. Thus, therapies aimed at curbing humoral autoimmunity while balancing immune competence are required. We propose that targeting key pathways involved in autoantibody development may be one such approach.

High affinity autoantibodies arise from GC reactions occurring in B cell follicles, following iterative rounds of somatic hypermutation of GC B cells and selection/maturation facilitated by T follicular B helper T cells (T_{FH}) [7]. GC B cells with high affinity for antigen eventually form antibody-producing plasma cells [10]. Accordingly, we reasoned that by targeting regulators of the GC reaction, the production of pathogenic autoantibodies could be limited, thereby inhibiting inflammation. Three target pathways are of relevance in this context. First, elevated type I IFN activity (the so-called type I IFN signature) is a remarkable feature of SLE, which can also be observed in some patients with RA and Sjögren's syndrome, and is associated with high-affinity autoantibodies, disease progression and poor prognosis [11, 12]. Type I IFN signalling through the common receptor IFNAR, can prime DCs to produce IL-6 in secondary lymphoid tissues. In turn, IL-6 supports the development of T_{FH} and Th17 in secondary lymphoid tissues, as well as the maintenance of terminally differentiated antibody-secreting plasma cells [13]. Third, the inducible T cell costimulator (ICOS) is required for the differentiation and maintenance of GC T_{FH}, which mediate GC interactions and facilitate antibody responses [14, 15, 16]. Loss or inhibition of these pathways has been shown to abrogate disease in humorally mediated autoimmune disease models [17, 18, 19, 20].

TANK-binding kinase 1 (TBK1) is an IKK-related Serine/Threonine kinase that is critical for the induction of IRF3-driven type I IFN responses in nucleic acid sensing pathways, such as TLR3/4-TRIF, RIG-I/MDA5-MAVS and cGAS-STING [21]. TBK1 also regulates IL-6 expression in response to TLR3 ligands [22] and to cytosolic DNA downstream of STING, but not to TLR9 ligands [23]. Because TBK1-/- mice are embryonic lethal, by using viable TBK1-/- TNF-/- mice [24] and STING-/- mice [23], TBK1-dependent induction of type I

IFNs and IL-6, respectively, have been shown to be required for humoral responses *in vivo*. TBK1 was also recently identified as a critical kinase for ICOS signalling in T_{FH} cells [25].

Given the involvement of TBK1 in regulating the production of type I IFNs and IL-6, as well as ICOS signalling, we hypothesized that TBK1 inhibition might provide an alternative approach to treatment of antibody-mediated inflammatory diseases. To explore this hypothesis, we generated WEHI-112 (a relatively selective small molecule inhibitor of TBK1) as a tool compound. TBK1 inhibition by WEHI-112 was confirmed by effective suppression of TRIF-TBK1-dependent IRF3 activation and IRF3-associated mediators in macrophage cell culture. *In vivo*, TBK1 inhibition alleviated the progression of established autoantibody-mediated CIA, but not the antibody-independent, antigen induced arthritis (AIA) model, nor the K/BxN serum transfer-induced arthritis (STIA) model. TBK1 inhibition reduced cytokine signalling and arthritogenic GC-driven humoral responses in CIA, in conjunction with lowered serum collagen type II (CII)-specific IgG1 levels. TBK1 inhibition may therefore provide an alternative therapeutic approach in RA and other autoantibody-mediated inflammatory diseases.

MATERIALS AND METHODS

Mice. Eight-to 10-week-old C57BL/6 and DBA/1 mice were obtained from WEHI Animal Supplies (Kew, Victoria, Australia). Mice were housed under standard conditions in the WEHI Animal Facility. All procedures were approved by the WEHI Animal Ethics Committee.

Chemical compounds. MRT67307 [26] was purchased from Sigma. Baricitinib (JAK2 inhibitor) was purchased from SelleckChem. WEHI-112 was synthesized at the Walter and Eliza Hall Institute. All compounds were dissolved in DMSO and diluted in 20% Captisol saline carrier solution.

Induction of arthritis and inhibitor treatment.

For CIA, DBA/1J mice were immunized intradermally with chicken type II collagen (CII) (2 mg/mL; Sigma-Aldrich) emulsified in an equal volume of CFA (containing 5 mg/mL heat-killed *Mycobacterium tuberculosis H37RA*, Difco Laboratories, Detroit, MI, USA) on day 0 and day 21. Intraperitoneal injection of vehicle or WEHI-112 (30 mg/kg) was initiated upon disease onset and mice were randomly enrolled into treatment and control groups.

For AIA, C57BL/6 mice were immunized intradermally with methylated BSA (mBSA) (2 mg/mL; Sigma-Aldrich) emulsified in an equal volume of CFA on day 0. Arthritis was induced on day 7 by an intraarticular injection of 200 µg mBSA in 10 µl of 0.9% w/v saline into the left knee. Intraperitoneal injection of vehicle or WEHI-112 (30 mg/kg) was initiated immediately

after intraarticular injection and mice were randomly enrolled into treatment or control groups.
For K/BxN STIA, C57BL/6 mice were injected with 100 ul serum from K/BxN mice on day 0. Intraperitoneal injection of vehicle or WEHI-112 (30 mg/kg) was initiated on day 1 and continued daily for 8 consecutive days.

Ag-specific Ab ELISA. Serial dilutions of sera were added to 96-well PolySorb microtiter plates (Nunc, ThermoFisher Scientific) coated with 5 µg/mL CII (Sigma-Aldrich) and incubated at room temperature for 2 h, followed by incubation with HRP-conjugated secondary antibodies against mouse IgG1 (1144-05), IgG2a (1155-05), IgG2b (1186-05), and IgM (1140-05) (Southern Biotechnology). The plates were developed with TMB substrate solution (BD Biosciences), and optical densities read at 450 nm. A mixture of sera from hyperimmunized DBA/1 mice with CIA was used to establish standard curves, and antibody levels are shown as relative titers.

Immunofluorescence. Lymph nodes were fixed in 4% PFA overnight, immersed in 20% sucrose for 1 h, embedded in TissueTek OCT compound and 8 µm cryostat sections were prepared. After blocking of non-specific binding sites with Avidin, Biotin and Protein block solutions (Dako) supplemented with 2.4G2 (100 µg/mL), sections were stained with Alexa Fluor 488-coupled GL7 (anti-GL7) and Alexa Fluor 647-coupled RA3-6B2 (anti-B220) (Biolegend). Nuclei were stained with DAPI. Whole lymph node sections were captured on an LSM 780 with ZEN2010 imaging software using the tile-scan function (Carl Zeiss).

T cell-restimulation assay. Primary CD4 T cell populations were isolated from pooled lymph nodes of DBA/1 mice with CIA. CD4 T cells were pre-gated as CD3+ CD4+ CD25- cells and sorted into $CD44^{hi}$ and $CD44^{int}$ populations. T cells were cultured in RPMI-1640 medium, supplemented with 10% FBS, glutamine, HEPES (10 mM), sodium pyruvate (1mM), β-mercaptoethanol, penicillin and streptomycin. Cells were left unstimulated or pre-conditioned with vehicle or WEHI-112 for 30 mins. Vehicle- or WEHI-112-treated cells were stimulated by combinations of purified endotoxin low and azide free anti-CD3 (3 µg/mL; 2C11 from Biolegend) and anti-ICOS (3 µg/mL; C398.4A from Biolegend). The antibodies were cross-linked at 37°C by goat antibody to hamster IgG (20 µg/mL; 127-005-099 from Jackson ImmunoResearch). For immunoblotting, cells were lysed in RIPA buffer after *in vitro* stimulation for 10 mins and the cell lysates probed for phospho-FoxO1 or β-actin by immunoblotting. For ImageStream analysis, sorted $CD44^{hi}$ cells were collected after stimulation for 30 mins, stained for total FoxO1 (C29H4) from Cell Signalling Technology,

counterstained with DAPI, acquired using AMNIS ImageStreamX MKII instrument, and analysed using the IDEAS software.

qRT-PCR. Total RNA was extracted from cells using ISOLATE II RNA Mini Kit (Bioline), digested with RNase-free DNase I (Bioline) and reverse transcribed into cDNA using superscript III (Invitrogen) using oligo-deoxy thymidine primers (Promega). Real-time qPCR was performed using Fast SYBR Green master mix (Thermo Fisher Scientific) and on a Viia7 PCR System (Thermo Fisher Scientific). Primers for the genes assessed are available in **Supplementary Table 1**. Gene expression levels were normalized to cellular GAPDH RNA levels.

Statistical analysis. Data are expressed as mean ± SEM. Statistical differences were assessed using the unpaired Student *t* test, paired Student *t* test, or one-way ANOVA Prism 6.0 software (GraphPad Software) as indicated. A P value ≤ 0.05 was considered statistically significant.

RESULTS

In vitro assessment of WEHI-112 as a TBK1 inhibitor.

Current pharmacological TBK1 inhibitors display off-target inhibition on other major kinases and some are poorly stable for in vivo use [26, 27]. We identified WEHI-112 as a lead compound of TBK1 inhibitor with improved selectivity and bioactivity. WEHI-112 potently inhibited TBK1 and its homolog IKKε (**Supplementary Table 2**), owing to a high degree of sequence homology. Cell-free biochemical assays revealed that WEHI-112 and literature standard TBK1 inhibitor MRT67307 [26] blocked TBK1 activity with a half-maximal inhibitory concentration (IC_{50}) of approximately 0.01 and 0.05 μM, respectively (**Figure 1A**). WEHI-112 and MRT67307 also inhibited IKKε activity at IC_{50} of 0.003 and 0.03 μM and JAK2 activity at 0.01 and 0.08 μM, respectively (**Figure 1A**). WEHI-112 and MRT67307 inhibited LPS-induced IRF3 phosphorylation of the TRIF-TBK1-IRF3 pathway in RAW264.7 macrophages (**Figure 1B**). In line with other TBK1 inhibitors, both WEHI-112 and MRT67307 paradoxically enhanced the phosphorylation of TBK1 and IKKε (**Figure 1B**), despite efficient inhibition of TBK1 activity [28]. The induction of TRIF-TBK1-IRF3-dependent genes (*Ifnb*, *Cxcl10*, and *Ccl5*) was reduced in LPS-induced macrophages in the presence of either WEHI-112 or MRT67307 (**Figure 1C**). WEHI-112 and MRT67307 did not affect the

induction of LPS-induced *Tnf* or *Il1b*, but suppressed *Il6* transcription in RAW264.7 macrophages (**Figure 1D**). Additionally, TBK1, rather than IKKε, was required for optimal *Il6* induction in response to LPS (**Figure 1E**). In summary, WEHI-112 is a potent and relatively selective inhibitor of TBK1.

WEHI-112 ameliorates T- and B cell-dependent CIA, but had minimal effect on B cell independent AIA, or T- and B- cell independent STIA.

To test the therapeutic potential of TBK1 inhibition using WEHI-112, we used the autoimmune CIA model of inflammatory arthritis. The CIA model is dependent on both cellular and humoral responses to collagen type II (CII) [29, 30]. Vehicle or WEHI-112 was administered immediately upon clinically evident signs of arthritis in immunised DBA/1 mice. Vehicle-treated mice developed progressive arthritis, but this was markedly inhibited in WEHI-112-treated mice (**Figure 2A**). Myeloperoxidase (MPO)-based IVIS imaging spectrum showed markedly attenuated inflammation in the limbs of mice treated with WEHI-112 (**Figure 2B**). Histological evaluation of the inflammatory cell influx, cartilage damage and bone degradation supported these observations (**Figures 2C-2D**). There were significant reductions in tissue-infiltrating neutrophils ($CD45^+$ $Ly6G^+$ $CD88^+$ CD64- $CD11b^+$) and macrophages ($CD45^+$ Ly6G- $CD88^+$ $CD64^+$ $CD11b^+$) (**Supplementary Figure 1**) in CIA mice treated with WEHI-112, relative to vehicle (**Figure 2E**).

WEHI-112 was next evaluated in the AIA model. AIA is T cell dependent, but independent of B cells and antibody production [31]. Vehicle or WEHI-112 was given immediately after intra-articular antigen challenge to induce AIA. WEHI-112 failed to inhibit inflammatory arthritis in the AIA model, as demonstrated by histology (**Figures 2F-2G**) and FACS analysis of the inflamed joint (**Figure 2H**). Additionally, WEHI-112 did not prevent the evolution of inflammatory arthritis in the K/BxN STIA model (which develops independently of adaptive immune mechanisms)[5], but may have had a modest effect on the severity of disease at later time points (**Figure 2I**). Collectively, these well described arthritis models show that WEHI-112 targets specific arthritogenic event(s) in CIA, to a much greater extent than AIA or STIA.

CIA development relies on efficient priming of humoral responses for the generation of arthritogenic CII-specific IgG1, and to a lesser extent, IgG2b autoantibodies [5]. Consistent with reduced arthritis, there was a significant reduction in pathogenic IgG1 anti-collagen antibodies and a modest reduction in IgG2b isotypes in WEHI-112-treated mice, compared to vehicle-treated mice. IgG2a and IgM anti-CII isotypes were not affected (**Figure 2J**).

Relative to naïve lymph nodes (LNs), there was no alteration in *Ifnb* or *Cxcl10* in CIA LNs (**Figure 2K**). In contrast, *Ccl5* was increased in CIA LNs relative to naïve LNs, but was reduced in CIA LNs upon treatment with WEHI-112 (**Figure 2K**). *Tnf*, *Il1b* and *Il6* were all

elevated in the CIA LNs compared to naïve LNs, but only *Il6* was reduced with WEHI-112 (**Figure 2L**), in line with reduced IL-6 induction *in vitro* with WEHI-112 or TBK1 deletion (**Figures 1D-1E**). Thus, the alleviation of CIA following TBK1 inhibition with WEHI-112 could be due to reduced levels of particular cytokines and chemokines in secondary lymphoid tissues.

Characterization of GC populations during the development of CIA.

Given the effect of WEHI-112 in reducing CII-specific IgG1 titers in CIA (**Figure 2J**), the importance of GC for development of CIA [32], and the requirement for TBK1 in mediating ICOS signalling during T_{FH} maturation [25], we examined the GC response following WEHI-112 treatment in the CIA model. Immunohistochemistry revealed an overall reduction in the GC size as determined by GC area relative to total LN size (**Figures 3A-3B**), although GC numbers were not affected by WEHI-112 (**Figure 3C**).

We defined mature GC T_{FH} as CD3+ CD4+ GL7+ cells and activated ICOS+ CD4 T cells as CD3+ CD4+ GL7- ICOS+ [33]. Compared to naïve mice, the LNs of mice with CIA had an expanded number of ICOS+ CD4+ T cells and GC T_{FH} cells (**Supplementary Figure 2A**). Upregulation of ICOS and GL7 expression in the DLNs of mice with active CIA was restricted to CD4+ T cells (**Supplementary Figure 2A**). GL7+ CD4+ GC T_{FH} cells had the highest expression of *Bcl6* (regulates T_{FH} differentiation and GC reactions), followed by GL7- ICOS+ CD4+ T cells and GL7- ICOS- CD4+ T cells (**Supplementary Figure 2B**). Markers of T_{FH} (*Cxcr5* and *Tnfsf5* (encodes CD40L)) were also higher in both GC T_{FH} and GL7- ICOS+ CD4 T cells (**Supplementary Figure 2B**), suggesting that the GL7- ICOS+ CD4 T cells likely contain pre-T_{FH} cells that have acquired CXCR5. *Il4* (for IgG1 class-switching) was exclusively enriched in the GC T_{FH} population (**Supplementary Figure 2C**), consistent with a previous report [34]. There was no difference in the expression level of *Il21* (for GC B cell proliferation) [35]. *Ifng* (for IgG2a class-switching) was enriched in both GC T_{FH} cells and ICOS+ CD4+ T cells, but no clear demarcation between the two subsets (**Supplementary Figure 2C**). *Csf2* (encodes GM-CSF) and *Il17a* (encodes IL-17) transcripts were less restricted to the GC T_{FH} population, compared to *Il4* (**Supplementary Figure 2C**). Thus, GL7 expression defines a population of IL-4-producing GC T_{FH} that might drive IL-4-dependent IgG1 responses in the LNs of mice with CIA. Indeed, ICOS-dependent GC T_{FH} cells have been shown to be indispensable for optimal maturation and selection of high-affinity IgG1 Abs via the secretion of IL-4 [34]. Complementary to the expanded GC T_{FH} population (**Supplementary Figure 2A**), LNs of mice with established CIA had an expanded CD19+ $GL7^{hi}$ GC B cell population (**Supplementary Figure 2D**). A large proportion of GC B cells from CIA LNs had undergone IgG1 class-switching, as these cells expressed membrane-bound IgG1 (IgG1+) and were actively cycling, as shown by BrdU uptake

(**Supplementary Figure 2E**) [35]. These GC B cells also exclusively expressed *Bcl6* (a master regulator of GC B cells) and *Aicda* (encoding activation-induced cytidine deaminase/AID for class switch recombination and somatic hypermutation) (**Supplementary Figure 2F**) [36].

WEHI-112 disrupts the established GC response in CIA.

TBK1-dependent ICOS signalling is required for GC T_{FH} differentiation from the pre-T_{FH} stage [25]. In turn, GC T_{FH} supports affinity maturation and selection of GC B cells for optimal production of high-affinity antibody [7, 37]. We examined if WEHI-112 impaired the differentiation of CD4+ T cell populations in reactive CIA LNs. WEHI-112 did not affect the frequency of GC $T_{FH,}$ nor of ICOS+ CD4 T cells during CIA (**Figures 4A-4B**). Nevertheless, the absolute numbers of both GC T_{FH} and ICOS+ CD4+ T cells (**Figure 4B**) were reduced. WEHI-112 did not alter the expression levels of *Il4*, *Il21*, or *Tnfsf5*, relative to T_{FH} cells taken from vehicle-treated mice (**Figure 4C**). However, *Ccr7* and *Sell* (encoding CD62L) were increased in T_{FH} from WEHI-112-treated mice (**Figure 4D**), suggesting relocation of GC T_{FH} away from the B follicle, and presumably towards the T cell zone [37, 38]. *Klf2* (a zinc-finger transcription factor, the down regulation of which is associated with the ICOS-dependent T_{FH} phenotype) and *Tbx21* (encoding the Th1-inducer T-bet transcription factor) were also increased in GC T_{FH} cells from WEHI-112-treated mice compared to control mice (**Figure 4D**), indicating phenotypic reversion to a pre-T_{FH} stage [15, 37, 38]. This pre-T_{FH} reversion has been noted with ICOSL blockade [15]. There was no obvious difference in *Bcl6*, *Cxcr4*, *S1p1r* or *Cxcr5* expression in the sorted GC T_{FH} cells (**Figure 4E**), consistent with CXCR5 induction being independent of ICOS [39]. *Bcl6* mRNA levels can be a poor indicator of Bcl6 expression [40]. We assessed changes in Bcl6 protein by flow cytometry, comparing WEHI-112 or Baricitinib (a JAK2/JAK1 inhibitor, which has negligible inhibitory activity towards TBK1)[41] to separate TBK1 and JAK2- mediated events seen with WEHI-112. WEHI-112 or Baricitinib were given for a short duration (4 days) to examine direct effects on GC responses. In line with gene expression profiling (**Supplementary Figure 2B**), GC T_{FH} (GL7+ ICOS+ CD4+) had the highest Bcl6 protein level, followed by GL7- ICOS+ CD4+, and GL7- ICOS- CD4+ T cell subsets (**Figure 4F**). WEHI-112, but not Baricitinib, reduced Bcl6 expression significantly in both GC T_{FH} and GL7- ICOS+ CD4+ T cells (**Figure 4F**). The suppression of Bcl6 by WEHI-112 most likely occurs through the inhibition of TBK1 downstream of ICOS signalling, consistent with Bcl6 induction being dependent on ICOS signalling [16]. The reduction of Bcl6 protein expression upon treatment WEHI-112 is also consistent with increased expression of mediators of T cell migration (*Ccr7* and *Sell*), as well as *Klf2* and *Tbx21*. This profile is suggestive of phenotypic reversion, as Bcl6 is known to repress programming of these alternative effector T cells [42]. Of note, both WEHI-112 and Baricitinib were able to suppress expression of osteoclast-associated genes, most notably

Mmp9 (**Supplementary Figure 3**). Altogether, these results also suggest that TBK1 inhibition with WEHI-112 suppressed the GC components while JAK inhibition alone may not be sufficient to exert such effect in the short period of time observed.

Sustained ICOS signalling is required for maintenance of the GC T_{FH} phenotype through the inactivation of FoxO1, as FoxO1 inhibits T_{FH} differentiation [14]. Inactivation of FoxO1 occurs through its phosphorylation, which induces cytosolic localization and thereby relieves the negative regulation of Bcl6 imposed by nuclear FoxO1 [14, 15]. We sorted CD3+ CD4+ CD25- cells T cells from the CIA LNs into $CD44^{hi}$ and $CD44^{int}$ populations. Consistent with published findings [43], engagement of ICOS enhanced phosphorylation of FoxO1 in $CD44^{hi}$ CD4 T cells, but not $CD44^{int}$ CD4 T cells (**Figure 5A**). WEHI-112 pre-treatment reduced ICOS-driven FoxO1 phosphorylation in $CD44^{hi}$ CD4 T cells (**Figure 5A**), consistent with maintenance of non-phosphorylated FoxO1 in the nucleus and negative regulation of Bcl6. This was also confirmed using ImageStream analysis. Total FoxO1 (in green) in unstimulated $CD44^{hi}$ CD4 T cells was mainly intranuclear (nuclear stain in purple). Agonistic anti-CD3 and anti-ICOS monoclonal antibodies induced FoxO1 cytoplasmic translocation, but nuclear egress was prevented in the presence of WEHI-112 (**Figures 5B and 5D**), without affecting overall FoxO1 expression (**Figure 5C**).

Proportion and absolute number of established secondary GC B cells were reduced with WEHI-112 treatment in CIA LNs (**Figure 6A**). Proliferative activity of the secondary GC B cells, however, was not altered (**Figure 6B**). Further supporting the possibility of phenotypic reversion of GC T_{FH}, sorted GC B cells from WEHI-112-treated CIA mice expressed lower mRNA levels of GC function regulators, *Aicda* and *Bcl6*, but not *Cxcr5*, relative to cells isolated from vehicle-treated mice (**Figure 6C**). Bcl6 protein in GC B cells was also reduced with WEHI-112, but not Baricitinib treatment (**Figure 6D**). These observations in the CIA model (**Figures 4-5**) are similar to the alterations of T_{FH} and GC B cell phenotypes following ICOSL blockade [15], as TBK1 inhibition with WEHI-112 resulted in the induction of chemokine receptor genes associated with alternative effector T cell fate. In agreement with GC size being directly linked with the magnitude and quality of humoral responses [44], inhibition of the GC reaction in CIA with WEHI-112 correlated with reduced arthritogenic antibody levels and a marked therapeutic effect on inflammatory arthritis.

DISCUSSION

Although the pathogenic sequence of events leading to breaches of immunological tolerance is likely to vary between RA patients, most patients have circulating, class-switched autoantibodies (e.g. ACPAs) and this is a well-documented risk factor for greater disease severity [45]. Therapeutic B cell-depletion using anti-CD20 antibody (Rituximab) underscores the importance of B cells in maintaining disease activity in RA. However,

Rituximab mainly targets short-lived antibody-secreting CD20+ plasma cells, leaving long-lived plasma cells intact [46]. GC-mediated somatic mutations and clonal selection are responsible for the generation of affinity-matured, autoantibody-producing long-lived plasma cells [7, 47, 48]. Thus, inhibition of ongoing GC that contributes to autoreactive plasma cell development offers therapeutic potential [3].

Optimal GC development and maintenance is positively regulated by type I IFNs, IL-6 and ICOS signalling [13, 14, 15, 16, 49, 50]. Because TBK1 is a common denominator of these pathways [24, 25], TBK1 inhibition might be therapeutically effective, even in established autoimmune diseases. To this end, we assessed the therapeutic use of a semi-selective lead compound - WEHI-112. We confirmed WEHI-112 as a TBK1 inhibitor *in vitro*, as it suppressed the induction of *Ifnb* and *Il6*. *In vivo*, WEHI-112 suppressed arthritis in autoantibody-dependent CIA, but had much less effect in T cell-mediated AIA or in the T- and B-independent K/BxN STIA model. The varied effects seen in these arthritis models indicate discrete immune mechanisms are differentially impacted by WEHI-112 treatment. CIA is a T cell- and B cell-dependent, GC-driven, autoantibody-mediated arthritis model, while the AIA model is entirely independent of the B cell compartment and antibody responses [29, 30, 31] and the STIA model is entirely independent of adaptive immune mechanisms[5]. Abrogated CIA was accompanied by reduced levels of arthritogenic, collagen-specific IgG1 and IgG2b isotypes, *Il6* and *Ccl5* expression, and GC size in reactive LNs. While IL-6 is well known for its importance in humoral responses and inflammation [13], CCL5 (RANTES) has not been extensively described in the context of humoral autoimmunity. Nevertheless, CCL5 blockade has been shown to reduce antigen-specific antibody responses through unknown mechanisms [51]. Although we could not detect type I IFN induction at the time point examined in CIA LNs, TBK1 inhibition has been shown to reduce the type I IFN signature and alleviate disease in the Trex1-/- murine model of SLE, through the inhibition of the cGAS-STING pathway [52]. Other reports demonstrate synergies between IL-6 and type I IFN by driving optimal T_{FH} polarization [50] and type I IFN-dependent IL-6 induction in DCs that supports GC-driven affinity maturation of antibodies [49]. Taken together, we propose that TBK1 inhibition reduces production of cytokines associated with humoral immunity, in particular IL-6, but likely type I IFNs as well.

The magnitude and quality of humoral responses is directly linked with GC size [44]. Consistent with this notion, inhibition of the GC reaction with WEHI-112 corresponded with reduced arthritogenic antibody levels and disease severity in CIA. Productive GC maintenance requires cooperative signals of GC T_{FH} and GC B cells through cytokines and costimulatory molecules [7, 48]. While the differentiation of naïve CD4 T cells into $Bcl6^{+}$ nascent T_{FH} requires ICOS-PI3K signalling, mature $Bcl6^{hi}$ GC T_{FH} differentiation and maintenance require ICOS/ICOSL signalling through TBK1 [15, 25]. Bcl6 maintains T_{FH} commitment by

repressing effector T cell programs [42]. We showed that GC T_{FH} from WEHI-112-treated CIA mice displayed phenotypic reversion towards an effector, Th1-like population, as indicated by the upregulation of *Tbx21*, *Ccr7* and *Sell* (which are normally repressed in T_{FH}) and accompanying reduction of Bcl6 protein expression. These findings are consistent with the re-acquisition of an effector T cell phenotype in the absence of ICOS/ICOSL signalling [15] and reduced Bcl6-mediated repression of effector T cell genes [42]. This effect of WEHI-112 on the GC response is most likely mediated through TBK1 inhibition, because in our hands, the JAK2 inhibitor Baricitinib did not alter Bcl6 expression in T_{FH} cells or GC B cells, although it did inhibit MMP9 expression to similar a degree in an osteoclastogenesis assay. Of note, conditional TBK1 deletion in CD4 T cells has been shown to augment effector Th1 responses, and renders these effector Th cells incapable of exiting the secondary lymphoid tissue in experimental autoimmune encephalomyelitis (EAE, a model of multiple sclerosis), due to the greatly enhanced expression of CCR7 and CD62L [53].

T_{FH} differentiation also requires FoxO1 inactivation downstream of ICOS [14]. WEHI-112 blocked ICOS-mediated phosphorylation and subsequent nuclear egress (inactivation) of FoxO1, in agreement with TBK1 being downstream of ICOS signalling [25]. Enforced nuclear retention of FoxO1 inhibits T_{FH} development through negative regulation of Bcl6 [14] and WEHI-112 recapitulated this phenotype. Complementing the changes in GC T_{FH} with WEHI-112, GC B cell responses were also abrogated in the CIA model. The effect of WEHI-112 in the CIA model resembles ICOSL blockade or deficiency, with reversion of the T_{FH} phenotype, dissolution of GCs and abrogation of downstream GC-dependent IgG antibody responses to T cell-dependent antigens [15]. It has been shown that even late-stage blockade of ICOSL-ICOS pathway ameliorates autoantibody driven disease models, including CIA, spontaneous K/BxN arthritis, proteoglycan-induced arthritis, (NZB/NZW) F1 lupus mice, and spontaneous lupus in the *Sanroque* mice [17, 18, 19]. Thus, TBK1 inhibition with WEHI-112 may recapitulate similar therapeutic effects of ICOSL blockade in humoral autoimmunity driven by GCs.

Although the effects of WEHI-112 observed in this study appear to be relatively selective to TBK1 inhibition and downstream cytokine and GC responses, it is important to note that WEHI-112 is not completely TBK1 selective, as it also targets IKKε and JAK2. The JAK2 inhibitor Baricitinib did not abrogate Bcl6 expression in GC T_{FH} and GC B cells, suggesting JAK2 inhibition is unlikely to explain the efficacy of WEHI-112 in the GC reaction of CIA. The observed effects on T_{FH} phenotype may also be mediated through IKKε pathway. However, we could not separate TBK1- and/or IKKε-mediated effects of WEHI-112 on the T_{FH} phenotype as there are no IKKε-specific inhibitors. Comparative studies using targeted deletion of TBK1 or IKKε in CD4 T cells would be of interest. Although these inhibitory activities on IKKε and JAK2 seem unlikely to explain the therapeutic effect of

WEHI-112, some inhibition of IKKε and JAK2 may actually provide synergistic therapeutic benefit. For example, IKKε appears to be involved in optimal Th17 function in response to IL-1β [54] and JAK2 is known to be downstream of several key inflammatory cytokines, such as IL-6, IL-12/23, GM-CSF and IFN-γ [55, 56]. Th17 cells in the early GC have been shown to modulate sialylation and thus the arthritogenicity of GC-derived autoantibodies [8]. In summary, we report WEHI-112 as a lead compound for TBK1 inhibitor and propose that TBK1 inhibition in RA, and potentially in other GC-associated humoral autoimmune diseases, may exert beneficial effects by reducing the pool of GC-derived, autoreactive long-lived PC and memory B cell populations, as well as inhibition of inflammatory cytokine signalling.

AUTHOR CONTRIBUTIONS

CL, DN, KEL, CJB and IPW designed and/or performed experiments. LP and CJB facilitated WEHI-112 production. HJ, PN and CJB supervised kinase and selectivity assays. DN and DS established the CRISPR cell line. CL and DD conducted in vitro validation of WEHI-112 and experiments on CRISPR cell lines. CL and DN performed arthritis experiments. DN performed IVIS imaging and histological analysis. CL and DN performed antibody ELISA assays. CL performed FACS analysis and cell sorting experiments. JH performed confocal microscopy. KEL supervised in vivo experiments and aided in manuscript assembly. CL, CJB and IPW wrote the manuscript.

ACKNOWLEDGEMENTS

This work was supported by the Reid Charitable Trusts, National Health and Medical Research Council of Australia Clinical Practitioner Fellowship (1023407), Program Grant (1016647) and Development Grant (1055374) and IRIISS (9000220), Victorian Government Operational Infrastructure Support, Australian Cancer Research Foundation and Dyson Bequest Funding (Dunn Fellowship to CJB).

REFERENCES

1. Smolen, J.S., Aletaha, D. & McInnes, I.B. Rheumatoid arthritis. *Lancet* **388**, 2023-2038 (2016).

2. Arbuckle, M.R. *et al.* Development of autoantibodies before the clinical onset of systemic lupus erythematosus. *N Engl J Med* **349**, 1526-1533 (2003).

3. Suurmond, J. & Diamond, B. Autoantibodies in systemic autoimmune diseases: specificity and pathogenicity. *J Clin Invest* **125**, 2194-2202 (2015).

4. Rutgers, A. *et al.* High affinity of anti-GBM antibodies from Goodpasture and transplanted Alport patients to alpha3(IV)NC1 collagen. *Kidney Int* **58**, 115-122 (2000).

5. Maccioni, M. *et al.* Arthritogenic monoclonal antibodies from K/BxN mice. *J Exp Med* **195**, 1071-1077 (2002).

6. Ji, H. *et al.* Critical roles for interleukin 1 and tumor necrosis factor alpha in antibody-induced arthritis. *J Exp Med* **196**, 77-85 (2002).

7. Ueno, H., Banchereau, J. & Vinuesa, C.G. Pathophysiology of T follicular helper cells in humans and mice. *Nat Immunol* **16**, 142-152 (2015).

8. Pfeifle, R. *et al.* Regulation of autoantibody activity by the IL-23-TH17 axis determines the onset of autoimmune disease. *Nat Immunol* **18**, 104-113 (2017).

9. Semerano, L., Minichiello, E., Bessis, N. & Boissier, M.C. Novel Immunotherapeutic Avenues for Rheumatoid Arthritis. *Trends Mol Med* **22**, 214-229 (2016).

10. Phan, T.G. *et al.* High affinity germinal center B cells are actively selected into the plasma cell compartment. *J Exp Med* **203**, 2419-2424 (2006).

11. Ronnblom, L., Alm, G.V. & Eloranta, M.L. Type I interferon and lupus. *Curr Opin Rheumatol* **21**, 471-477 (2009).

12. Nordmark, G., Eloranta, M.L. & Ronnblom, L. Primary Sjogren's syndrome and the type I interferon system. *Curr Pharm Biotechnol* **13**, 2054-2062 (2012).

13. Hunter, C.A. & Jones, S.A. IL-6 as a keystone cytokine in health and disease. *Nat Immunol* **16**, 448-457 (2015).

14. Stone, E.L. *et al.* ICOS coreceptor signaling inactivates the transcription factor FOXO1 to promote Tfh cell differentiation. *Immunity* **42**, 239-251 (2015).

15. Weber, J.P. *et al.* ICOS maintains the T follicular helper cell phenotype by down-regulating Kruppel-like factor 2. *J Exp Med* **212**, 217-233 (2015).

16. Choi, Y.S. *et al.* ICOS receptor instructs T follicular helper cell versus effector cell differentiation via induction of the transcriptional repressor Bcl6. *Immunity* **34**, 932-946 (2011).

17. Hamel, K.M., Cao, Y., Olalekan, S.A. & Finnegan, A. B cell-specific expression of inducible costimulator ligand is necessary for the induction of arthritis in mice. *Arthritis Rheumatol* **66**, 60-67 (2014).

18. Hu, Y.L., Metz, D.P., Chung, J., Siu, G. & Zhang, M. B7RP-1 blockade ameliorates autoimmunity through regulation of follicular helper T cells. *J Immunol* **182**, 1421-1428 (2009).

19. Iwai, H. *et al.* Amelioration of collagen-induced arthritis by blockade of inducible costimulator-B7 homologous protein costimulation. *J Immunol* **169**, 4332-4339 (2002).

20. Wong, S.C., Oh, E., Ng, C.H. & Lam, K.P. Impaired germinal center formation and recall T-cell-dependent immune responses in mice lacking the costimulatory ligand B7-H2. *Blood* **102**, 1381-1388 (2003).

21. Liu, S. *et al.* Phosphorylation of innate immune adaptor proteins MAVS, STING, and TRIF induces IRF3 activation. *Science* **347**, aaa2630 (2015).

22. Herman, M. *et al.* Heterozygous TBK1 mutations impair TLR3 immunity and underlie herpes simplex encephalitis of childhood. *J Exp Med* **209**, 1567-1582 (2012).

23. Ishikawa, H., Ma, Z. & Barber, G.N. STING regulates intracellular DNA-mediated, type I interferon-dependent innate immunity. *Nature* **461**, 788-792 (2009).

24. Ishii, K.J. *et al.* TANK-binding kinase-1 delineates innate and adaptive immune responses to DNA vaccines. *Nature* **451**, 725-729 (2008).

25. Pedros, C. *et al.* A TRAF-like motif of the inducible costimulator ICOS controls development of germinal center TFH cells via the kinase TBK1. *Nat Immunol* **17**, 825-833 (2016).

26. Clark, K. *et al.* Novel cross-talk within the IKK family controls innate immunity. *Biochem J* **434**, 93-104 (2011).

27. Reilly, S.M. *et al.* An inhibitor of the protein kinases TBK1 and IKK-varepsilon improves obesity-related metabolic dysfunctions in mice. *Nat Med* **19**, 313-321 (2013).

28. Clark, K., Plater, L., Peggie, M. & Cohen, P. Use of the pharmacological inhibitor BX795 to study the regulation and physiological roles of TBK1 and IkappaB kinase epsilon: a distinct upstream kinase mediates Ser-172 phosphorylation and activation. *J Biol Chem* **284**, 14136-14146 (2009).

29. Svensson, L., Jirholt, J., Holmdahl, R. & Jansson, L. B cell-deficient mice do not develop type II collagen-induced arthritis (CIA). *Clin Exp Immunol* **111**, 521-526 (1998).

30. Corthay, A., Johansson, A., Vestberg, M. & Holmdahl, R. Collagen-induced arthritis development requires alpha beta T cells but not gamma delta T cells: studies with T cell-deficient (TCR mutant) mice. *Int Immunol* **11**, 1065-1073 (1999).

31. Wong, P.K. *et al.* Interleukin-6 modulates production of T lymphocyte-derived cytokines in antigen-induced arthritis and drives inflammation-induced osteoclastogenesis. *Arthritis Rheum* **54**, 158-168 (2006).

32. Dahdah, A. *et al.* Germinal center B cells are essential for collagen-induced arthritis. *Arthritis Rheumatol* (2017).

33. Kerfoot, S.M. *et al.* Germinal center B cell and T follicular helper cell development initiates in the interfollicular zone. *Immunity* **34**, 947-960 (2011).

34. Reinhardt, R.L., Liang, H.E. & Locksley, R.M. Cytokine-secreting follicular T cells shape the antibody repertoire. *Nat Immunol* **10**, 385-393 (2009).

35. Zotos, D. *et al.* IL-21 regulates germinal center B cell differentiation and proliferation through a B cell-intrinsic mechanism. *J Exp Med* **207**, 365-378 (2010).

36. Basso, K. *et al.* BCL6 positively regulates AID and germinal center gene expression via repression of miR-155. *J Exp Med* **209**, 2455-2465 (2012).

37. Hardtke, S., Ohl, L. & Forster, R. Balanced expression of CXCR5 and CCR7 on follicular T helper cells determines their transient positioning to lymph node follicles and is essential for efficient B-cell help. *Blood* **106**, 1924-1931 (2005).

38. Haynes, N.M. *et al.* Role of CXCR5 and CCR7 in follicular Th cell positioning and appearance of a programmed cell death gene-1high germinal center-associated subpopulation. *J Immunol* **179**, 5099-5108 (2007).

39. Odegard, J.M. *et al.* ICOS-dependent extrafollicular helper T cells elicit IgG production via IL-21 in systemic autoimmunity. *J Exp Med* **205**, 2873-2886 (2008).

40. Kitano, M. *et al.* Bcl6 protein expression shapes pre-germinal center B cell dynamics and follicular helper T cell heterogeneity. *Immunity* **34**, 961-972 (2011).

41. Klaeger, S. *et al.* The target landscape of clinical kinase drugs. *Science* **358** (2017).

42. Hatzi, K. *et al.* BCL6 orchestrates Tfh cell differentiation via multiple distinct mechanisms. *J Exp Med* **212**, 539-553 (2015).

43. Xiao, N. *et al.* The E3 ubiquitin ligase Itch is required for the differentiation of follicular helper T cells. *Nat Immunol* **15**, 657-666 (2014).

44. Baumjohann, D. *et al.* Persistent antigen and germinal center B cells sustain T follicular helper cell responses and phenotype. *Immunity* **38**, 596-605 (2013).

45. Willemze, A., Trouw, L.A., Toes, R.E. & Huizinga, T.W. The influence of ACPA status and characteristics on the course of RA. *Nat Rev Rheumatol* **8**, 144-152 (2012).

46. Huang, H., Benoist, C. & Mathis, D. Rituximab specifically depletes short-lived autoreactive plasma cells in a mouse model of inflammatory arthritis. *Proc Natl Acad Sci U S A* **107**, 4658-4663 (2010).

47. Hiepe, F. *et al.* Long-lived autoreactive plasma cells drive persistent autoimmune inflammation. *Nat Rev Rheumatol* **7**, 170-178 (2011).

48. Victora, G.D. & Nussenzweig, M.C. Germinal centers. *Annu Rev Immunol* **30**, 429-457 (2012).

49. Cucak, H., Yrlid, U., Reizis, B., Kalinke, U. & Johansson-Lindbom, B. Type I interferon signaling in dendritic cells stimulates the development of lymph-node-resident T follicular helper cells. *Immunity* **31**, 491-501 (2009).

50. Riteau, N. *et al.* Water-in-Oil-Only Adjuvants Selectively Promote T Follicular Helper Cell Polarization through a Type I IFN and IL-6-Dependent Pathway. *J Immunol* **197**, 3884-3893 (2016).

51. Palaniappan, R. *et al.* CCL5 modulates pneumococcal immunity and carriage. *J Immunol* **176**, 2346-2356 (2006).

52. Hasan, M. *et al.* Cutting Edge: Inhibiting TBK1 by Compound II Ameliorates Autoimmune Disease in Mice. *J Immunol* **195**, 4573-4577 (2015).

53. Yu, J. *et al.* Regulation of T-cell activation and migration by the kinase TBK1 during neuroinflammation. *Nat Commun* **6**, 6074 (2015).

54. Gulen, M.F. *et al.* Inactivation of the enzyme GSK3alpha by the kinase IKKi promotes AKT-mTOR signaling pathway that mediates interleukin-1-induced Th17 cell maintenance. *Immunity* **37**, 800-812 (2012).

55. O'Shea, J.J., Kontzias, A., Yamaoka, K., Tanaka, Y. & Laurence, A. Janus kinase inhibitors in autoimmune diseases. *Ann Rheum Dis* **72 Suppl 2**, ii111-115 (2013).

56. Schwartz, D.M., Bonelli, M., Gadina, M. & O'Shea, J.J. Type I/II cytokines, JAKs, and new strategies for treating autoimmune diseases. *Nat Rev Rheumatol* **12**, 25-36 (2016).

FIGURE LEGENDS

Figure 1. WEHI-112 is a potent inhibitor of TBK1. (A) Dose-response curves showing inhibition of TBK1, IKKε and JAK2 kinase activity in the presence of WEHI-112 or MRT67307. Percentage activity was calculated using the no inhibitor control as 100% activity. Data show a representative from two independent experiments. (B) Immunoblot analysis of phosphorylated (P-) IRF3, TBK1 and IKKε in whole-cell lysates of RAW264.7 macrophages that were preconditioned with vehicle, 0.25 μM WEHI-112, or 0.25 μM MRT67307 for 1 h prior to 1.5 h stimulation with LPS (0.1 μg/mL). Data show a representative experiment from two independent experiments. (C-D) Real-time PCR analysis of (C) *Ifnb*, *Cxcl10* and *Ccl5*, and (D) *Tnf*, *Il1b* and *Il6* in RAW264.7 macrophages left unstimulated (US) or preconditioned with vehicle or 0.25 μM inhibitor (WEHI-112, MRT67307) for 1 h followed by stimulation for 4 h with LPS (0.1 μg/mL). Data are pooled from five independent experiments. Mean ± SEM (Student's t-test: US or inhibitor versus vehicle; ** P<0.01, *** P<0.005). (E) Real-time PCR analysis of *Tnf*, *Il1b* and *Il6* in THP-1 human monocyte-derived macrophages that were stimulated for 4 h with LPS (0.1 μg/mL) following CRISPR-Cas9-mediated deletion of endogenous TBK1 or IKKε. Data are pooled from five independent experiments. Mean ± SEM (Student's t-test: Control versus TBK1 KO or IKKε KO; * P<0.05).

Figure 2. WEHI-112 markedly inhibits the progression of established CIA, but has minimal effects on AIA or STIA. (A-E, J-L) DBA/1 mice with CIA were randomly enrolled into treatment or control groups at arthritis onset (day 1) to receive WEHI-112 (30 mg/kg) or vehicle i.p. daily for 7 days. (A) Mice were evaluated daily for clinical features of CIA. Data are pooled from four independent experiments with 4-5 mice per group per experiment. Mean ± SEM (Student's t-test: WEHI-112 versus vehicle; ** P<0.01, **** P<0.0001). (B)

Representative bioluminescent images and quantification of MPO activity in arthritic DBA/1 (described in 2A) at indicated times. Mean ± SEM (Student's t-test: WEHI-112 versus vehicle; * P<0.05). (C) Representative Safranin-O staining of histological joint sections from CIA mice treated with vehicle or WEHI-112. (D) Histological evaluation of total arthritis clinical scores. Error bars represent SEM. (E) Quantification of joint infiltrating neutrophils and macrophages in the ankle joints of DBA/1 CIA mice. (F-H) C57BL/6 mice were immunized with antigen methylated BSA (mBSA) in CFA on day 0. Arthritis was induced by an intraarticular injection of mBSA into the knee on day 7. Vehicle or WEHI-112 was given daily i.p. from day 7 to 13 and knee joints were collected for analysis on day 14. (F) Representative Safranin-O staining of histological joint sections from AIA mice treated with vehicle or WEHI-112. (G) Macroscopic score of histological changes in affected AIA knee joints (0 = normal, 1 = mild, 2 = moderate, 3 = severe). Data are pooled from two independent experiments with 4-5 mice per group per experiment. (H) Quantification of joint infiltrating neutrophils and macrophages in the knee joints of C57BL/6 AIA mice. Data are pooled from two independent experiments with 4-5 mice per group per experiment. Mean ± SEM. (I) Clinical arthritis severity in C57BL/6 mice receiving K/BxN serum on day 0 (STIA), followed by WEHI-112 or vehicle i.p daily for the next 8 days. Data are pooled from two independent experiments with 4-5 mice per group, per experiment. (J) ELISA of immunoglobulin isotypes specific for CII in the serum from CIA mice collected at endpoint. Data are pooled from three independent experiments (Student's t-test: WEHI-112 versus vehicle: * P<0.05, *** P<0.005). (K-L) Real-time PCR analysis of (K) *Ifnb*, *Cxcl10* and *Ccl5*, and (L) *Tnf*, *Il1b* and *Il6* in total LN cells derived from CIA mice. Data are representative from two independent experiments. Mean ± SEM (Student's t-test: US or inhibitor versus vehicle; * P<0.05, ** P<0.01).

Figure 3. WEHI-112 treatment contracts the established GC response. DBA/1 CIA mice were randomly enrolled into treatment or control groups at arthritis onset. WEHI-112 (30 mg/kg) was given daily for the next 4 days. GCs were analysed by immunofluorescence analysis of DLNs on day 34. The B cells (B220+) are shown in red, GC cells (GL7+) in green and nuclear DAPI stain in blue. (A) Representative images of whole lymph node sections from CIA mice treated with vehicle or WEHI-112, showing GCs in green. (B) Quantification of GC size (GC area relative to total LN area) and (C) numbers of GC per LN. Data are representative of two experiments with 4-5 mice per group per experiment. Mean ± SEM (Student's t-test: WEHI-112 versus vehicle; ** P<0.01).

Figure 4. Reversal of the GC T_{FH} phenotype with WEHI-112. DBA/1 CIA mice were randomly enrolled into treatment or control groups at arthritis onset. (A-E) Vehicle or WEHI-

112 (30 mg/kg) was given daily for the next 4 days. GC T_{FH} and ICOS+ CD4 T cells in the DLNs were analysed by flow cytometry. (A) Representative flow cytometry plots indicating the frequency of GL7+ GC T_{FH} and $ICOS^+$ populations among CD4+ T cells. (B) Frequency and numbers of GL7+ GC T_{FH} cells (*top*) and $ICOS^+$ $CD4^+$ T cells (*bottom*). (C-E) Real-time PCR analysis of T_{FH}-associated genes in sorted GL7+ GC T_{FH} cells isolated from vehicle- or WEHI-112-treated LNs. Data are from two experiments with 3-4 mice per group per experiment. Mean ± SEM (Student's t-test: WEHI-112 versus vehicle; * P<0.05, ** P<0.01, *** P<0.005). (F) Vehicle, WEHI-112, or Baricitinib (30 mg/kg) was given daily for the next 4 days. MFI of Bcl6 on gated CD4+ T cells populations from LNs of mice treated with vehicle, WEHI-112 or Baricitinib. Data are from two experiments with 3-4 mice per group per experiment.

Figure 5. WEHI-112 inhibits ICOS-mediated FoxO1 phosphorylation and inactivation. (A) Immunoblot analysis of lysates of CD4 T cell populations ($CD44^{hi}$ or $CD44^{int}$) sorted as CD3+ CD4+ CD25- from LNs of DBA/1 mice with CIA. Sorted cells were cultured and left unstimulated (US), or pre-treated with vehicle or WEHI-112 for 30 mins and stimulated with anti-CD3 (3 µg/mL) and anti-ICOS (3 µg/mL) for 10 mins. Data are representative of two independent experiments. (B) ImageStream analysis of CD4+ $CD44^{hi}$ T cells sorted as CD3+ CD4+ CD25- from LNs of DBA/1 mice with CIA. Sorted cells were cultured and conditioned as in A then restimulated with anti-CD3 and anti-ICOS for 30 mins. (C) MFI of FoxO1-GFP and (D) similarity score between DAPI and FoxO1-GFP. Data are representative of two independent experiments. (B-D) Data are representative of two independent experiments, performed in quadruplicate in each experiment. Mean ± SEM (Student's t-test: WEHI-112 versus vehicle; ** P<0.01, *** P<0.005).

Figure 6. WEHI-112 disrupts the established GC B cell response. DBA/1 CIA mice were randomly enrolled at arthritis onset into treatment or control groups. Vehicle or WEHI-112 (30 mg/kg) was given daily for the next 4 days. GC B cells in the LNs were analysed by flow cytometry. (A) Representative flow cytometry plots and bar graph indicating the frequency of GL7+ GC B cells among CD19+ B cells, and numbers of GL7+ GC B cells. (B) Representative flow cytometry plots and bar graph indicating the frequency of BrdU+ cells among GC B cells. (C) Real-time PCR analysis of GC-associated genes in sorted GL7+ GC B cells isolated from LNs of mice treated with vehicle or WEHI-112 treated. (D) MFI of Bcl6 on gated GC B cells from LNs of mice treated with vehicle, WEHI-112 or Baricitinib. Data are from two experiments with 3-4 mice per group per experiment. Mean ± SEM (Student's t-test: WEHI-112 versus vehicle; ** P<0.01, *** P<0.005).

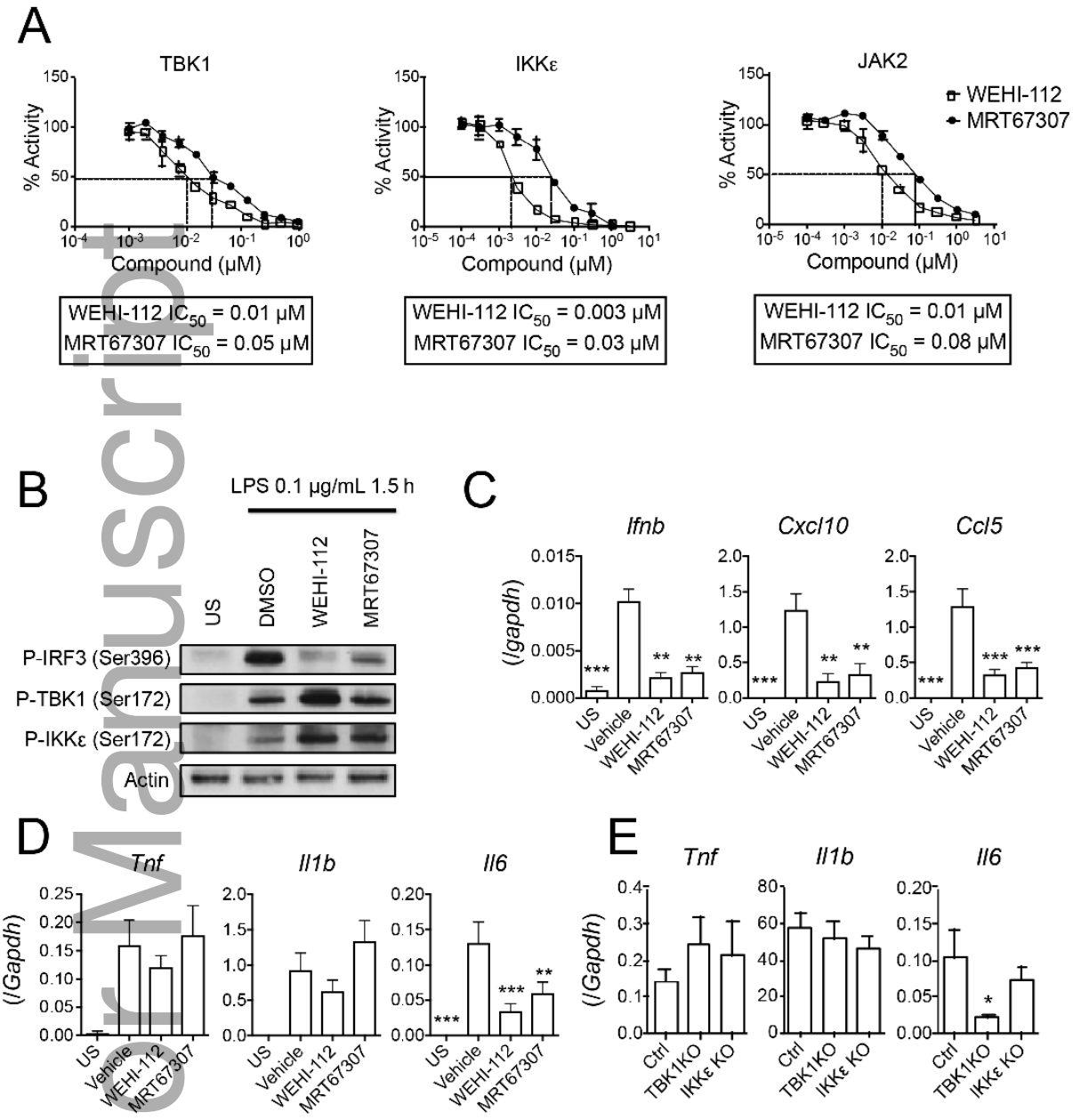

art_40670_f1.tiff

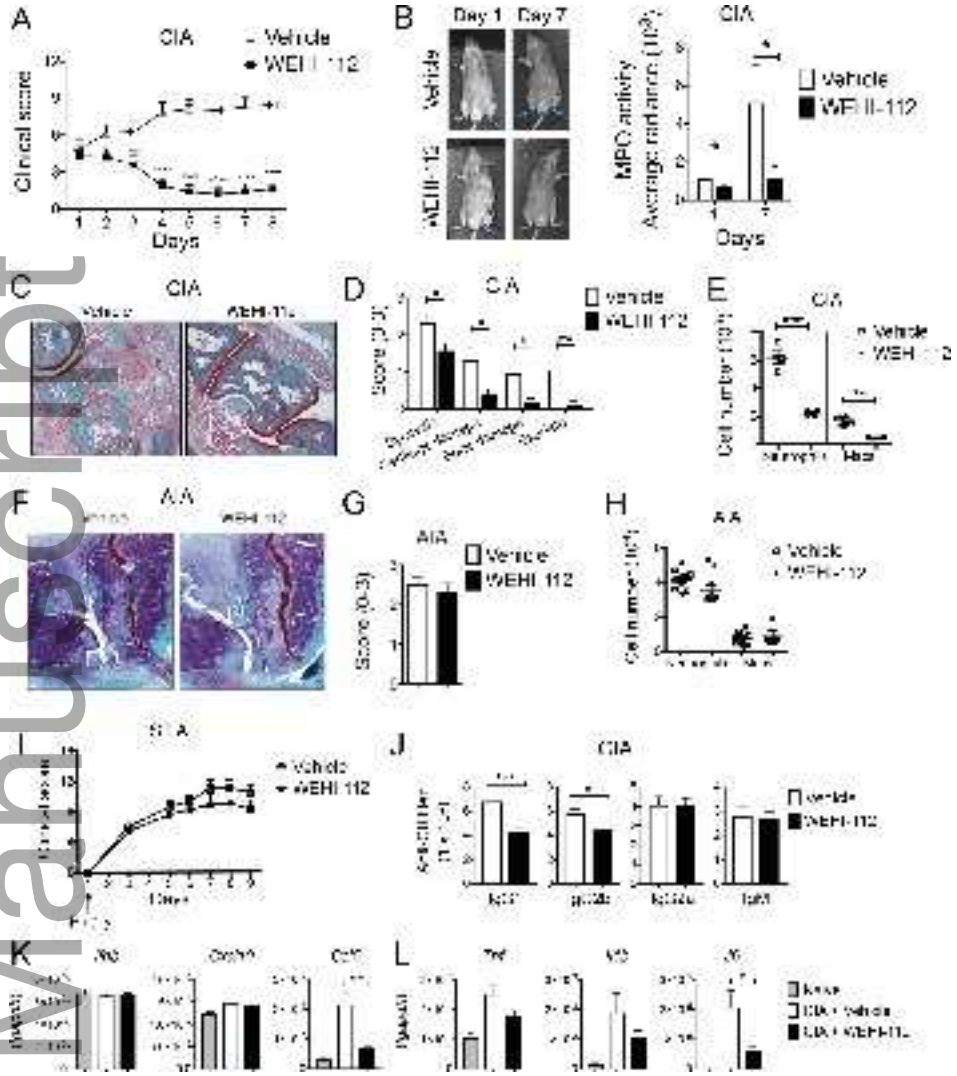

art_40670_f2.tiff

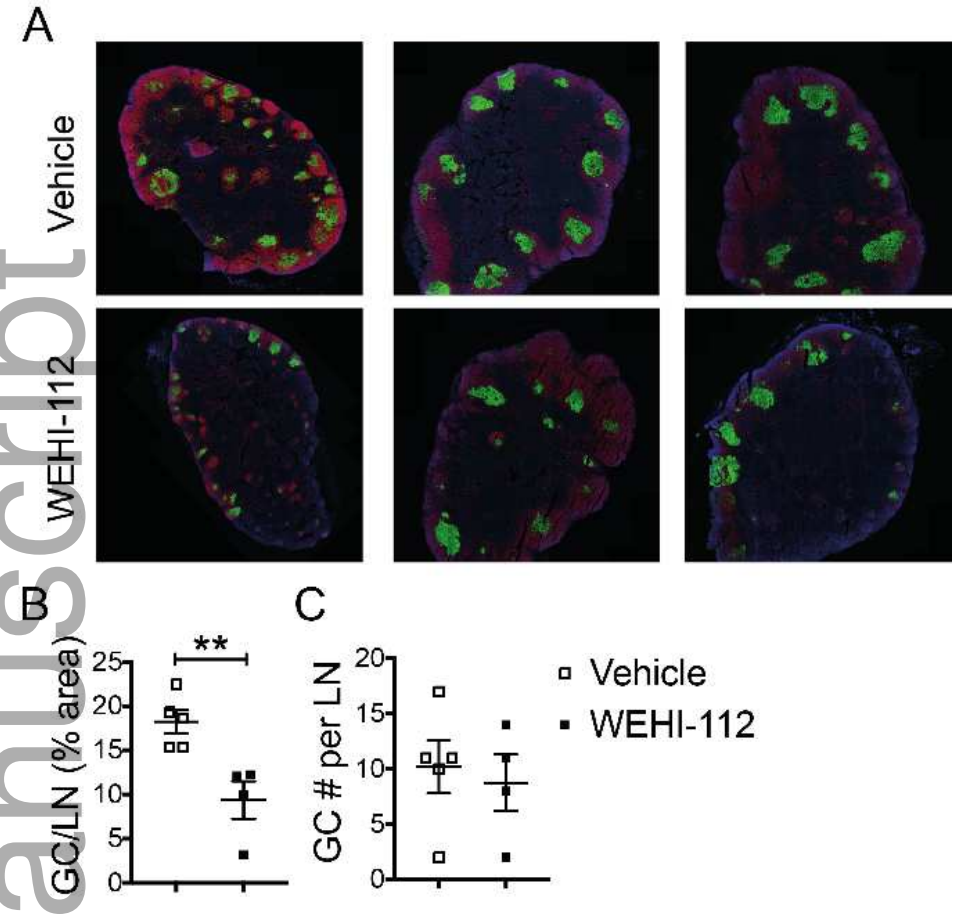

art_40670_f3.tiff

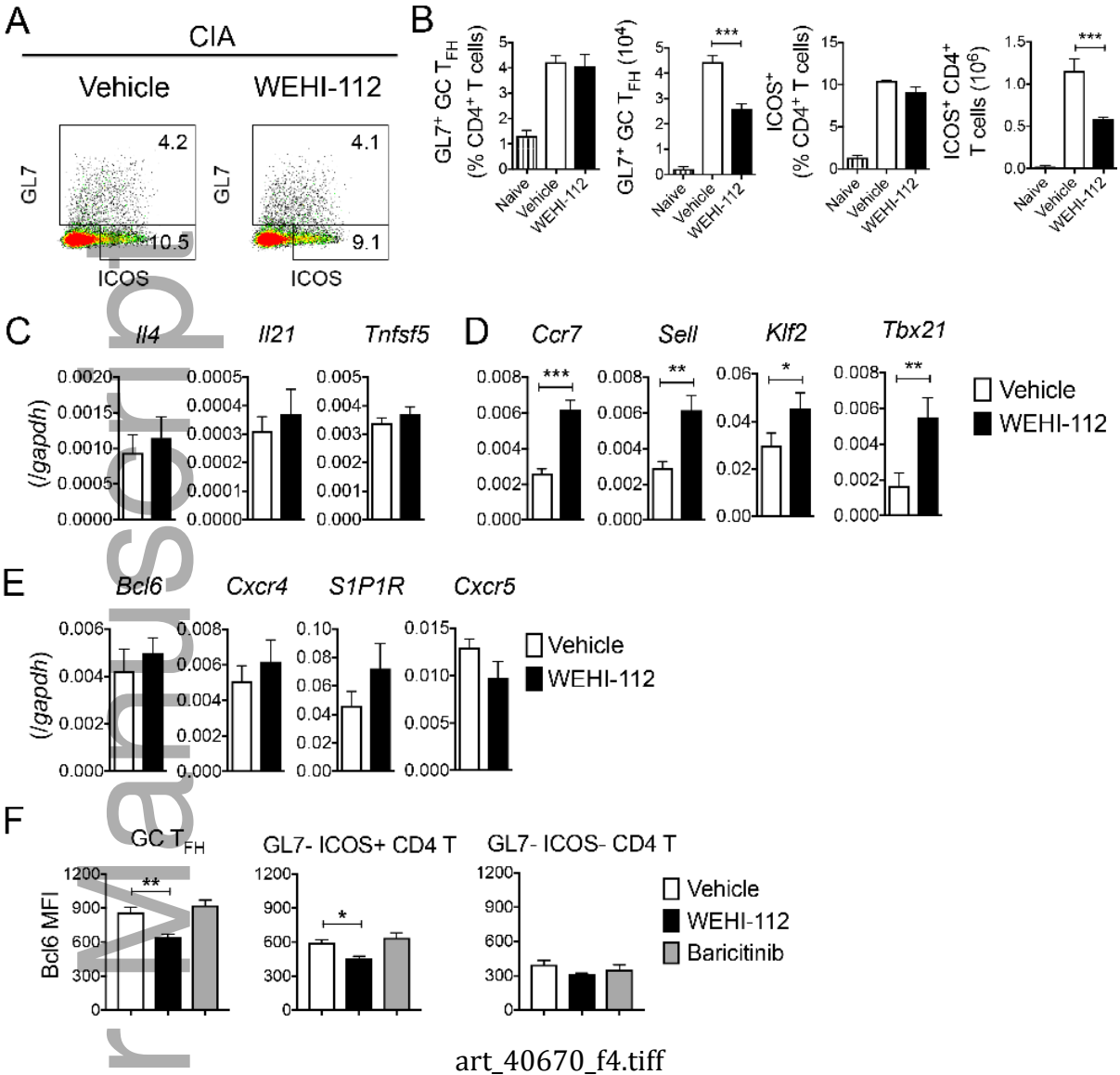

art_40670_f4.tiff

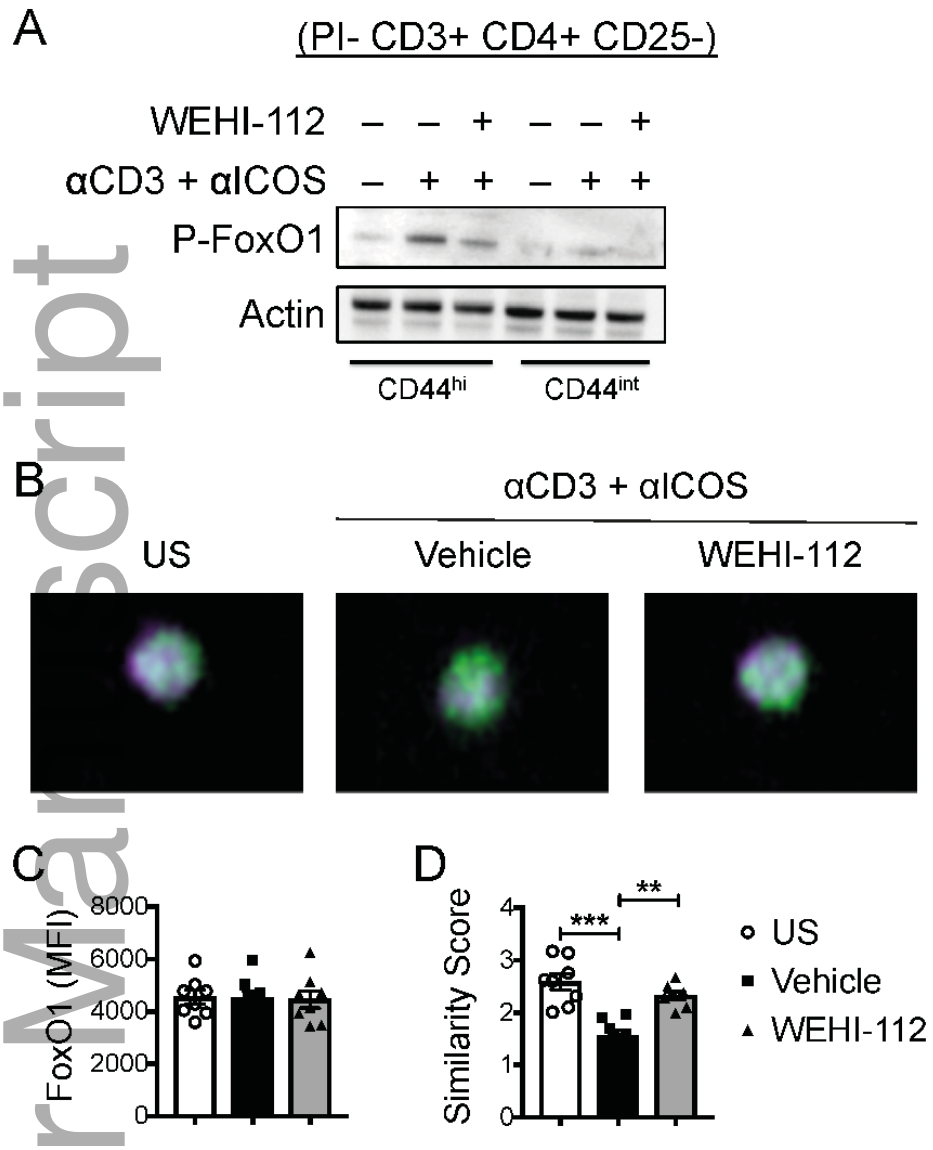

art_40670_f5.tiff

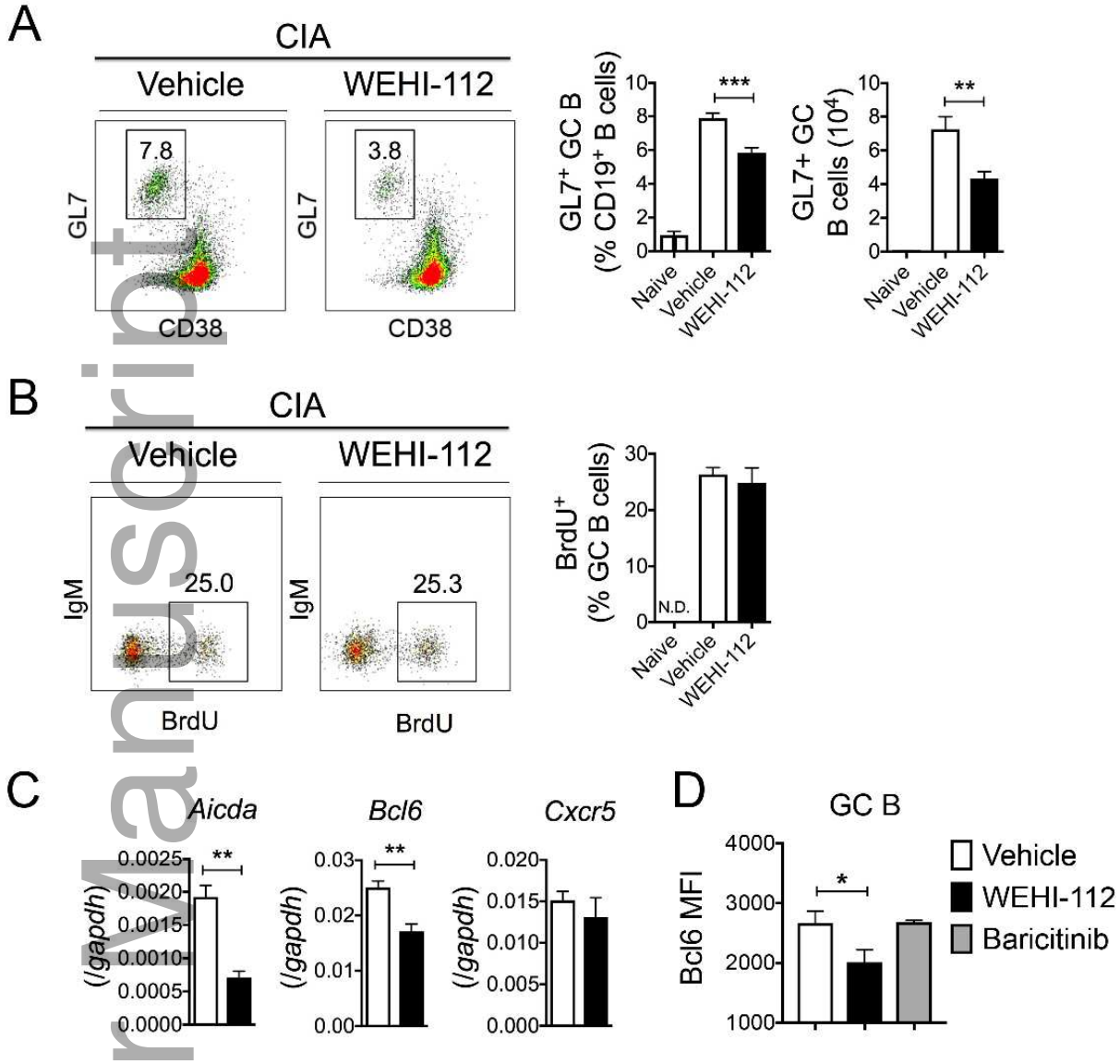

art_40670_f6.tiff